Perturbative Analysis on a Lunar Free Return Trajectory

Emre Ünal, Hasan Başaran

Abstract—In this study, starting with a predetermined Lunar free-return trajectory, an analysis of major near-Earth perturbations is carried out. Referencing to historical Apollo-13 flight, changes in the mission's resultant perimoon and perigee altitudes with each perturbative effect are evaluated. The perturbations that were considered are Earth oblateness effects, up to the 6th order, atmospheric drag, third body perturbations consisting of solar and planetary effects and solar radiation pressure effects. It is found that for a Moon mission, most of the main perturbative effects spoil the trajectory significantly while some came out to be negligible. It is seen that for apparent future request of constructing low cost, reliable and safe trajectories to the Moon, most of the orbital perturbations are crucial.

Keywords—Apollo-13 trajectory, atmospheric drag, lunar trajectories, oblateness effect, perturbative effects, solar radiation pressure, third body perturbations.

I. INTRODUCTION

HUMANITY began their space journey back in the 1900s. According to some, it was the beginning of the space era when Sputnik-1 was inserted into orbit in 1957. Starting with the low earth orbit satellites, in the space era, Earth's very natural satellite Moon, Mars, Jupiter and even the boundaries of the solar system have been reached. Since then, plans and goals have changed, and after half a century since man's first step on Moon, once again plans are being made to return, but with essential differences in the goals of the mission. Recently, building an outpost was suggested as one of the primary objectives of returning to the Moon. Space mining, since the Moon itself has large Helium-3 reservoirs which results from the harsh bombardment by solar wind due to weak magnetic field of the Moon, is another major goal [1]. Also, the Moon is a unique place for telescopes. It will provide improved deep space observations since its rotation period around itself is equal to its orbital period around the Earth, approximately 27 days. Compared to the telescopes orbiting around the Earth, inertial stabilization of the lunar surface telescopes is much easier. In addition, particle density on the lunar surface is one millionth of that of Hubble's altitude; hence, the clarity of the observations will be much better [2]. Another important goal is facilitating deep space missions. The Moon is a distant object to the Earth and has relatively low gravity, thus, reaching the escape velocity for interplanetary missions is much easier from the lunar surface.

E. Ünal is with Roketsan Inc., Flight Mechanics Tech. Dept., Ankara, CO 06780, Turkey (corresponding author, e-mail: emre.unal@roketsan.com.tr).

H. Başaran is with Roketsan Inc., Flight Mechanics Tech. Dept., Ankara, CO 06780, Turkey (e-mail: hasan.basaran@roketsan.com.tr).

Moreover, launches can be conducted using catapult-like systems, more specifically electromagnetic rail guns, owing to the atmosphere free environment [3]. Additionally, examination of the mineral composition [4], performing a terrain mapping of the Moon for navigation purposes [4], examination of the ice deposits located in the permanently dark craters [5] and the investigation of the geophysical nodes to construct a seismic network on the Moon in order to study its evolution and the Moon-quakes [6] are listed as the other recent goals.

A. Related Work

In regard with the Lunar trajectories, Adamo has used state transition matrices to reconstruct the Apollo-13 mission trajectory [7]. Jesick and Ocampo presented an automated lunar free-return trajectory generation procedure [8]. Li et al. studied two-segment lunar free return trajectories to save fuel and provided initial solutions [9]. Unal constructed lunar free-return trajectories with several methods discussing pros and cons of them [10].

Perturbative analysis will be held on the trajectory evaluated in his work. Referencing to Apollo-13 flight trajectory, it will be discussed in this paper how perturbations effect a free-return path. Starting with a predetermined free-return trajectory, Earth oblateness, atmospheric drag, third body perturbations and solar radiation pressure effects will be analyzed. In conclusion, the perturbations that should be considered for a Moon mission will be decided.

B. Apollo-13 and the Reference Free-Return Trajectory

The USA faced a lethal problem in 1970 during the Apollo-13 mission. The malfunction was an explosion of an oxygen tank which damaged a valve or ruptured a line in another oxygen tank, causing it to be out of order together with it in the service module. Having lost two oxygen tanks, the mission was cancelled in the 3rd day of the flight, as the sequence of events can be seen in Fig. 1. The mission crew safely made it back to the Earth with the aid of free-return phenomena and mission planners who have designed the trajectory in accordance with it. Along the trajectory, the spacecraft enters the Lunar sphere of influence (SOI), flies around the Moon and turns back to Earth.

Starting from the Apollo-13 initial parameters, excluding perturbative effects, Unal has found similar resultant altitudes with proper tolerance levels. Apollo-13 and its trajectory parameters are represented in Table I [7]−[10]. Also, the trajectory is shown in Figs. 2 and 3 in the Earth & Moon center-of-mass (COM) centered frame and Moon centered frame, respectively.
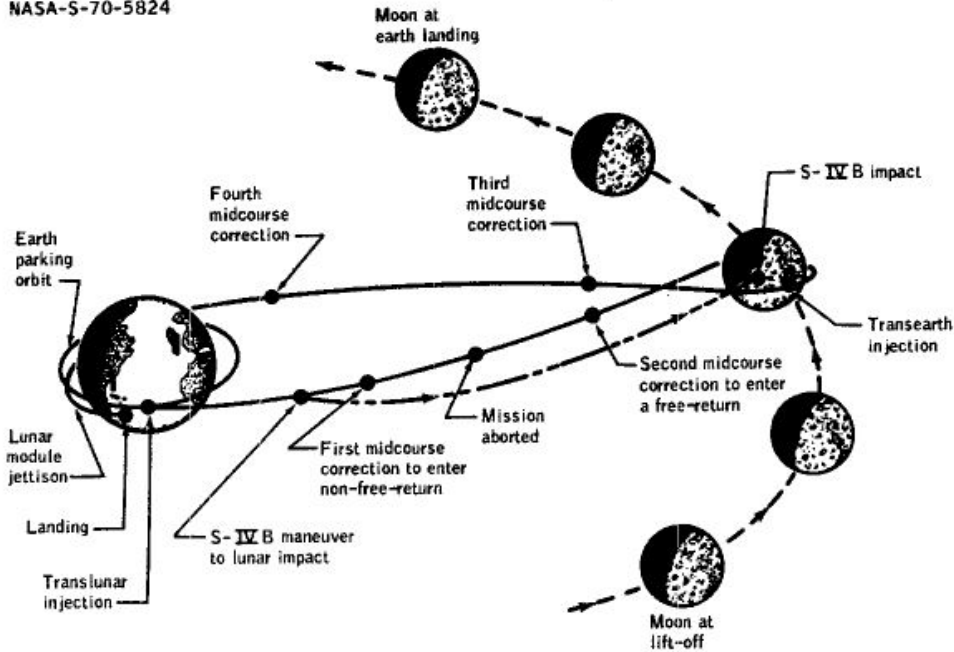
Fig. 1 Apollo-13 Trajectory [11]

TABLE I
APOLLO-13 AND REFERENCE TRAJECTORY PARAMETERS

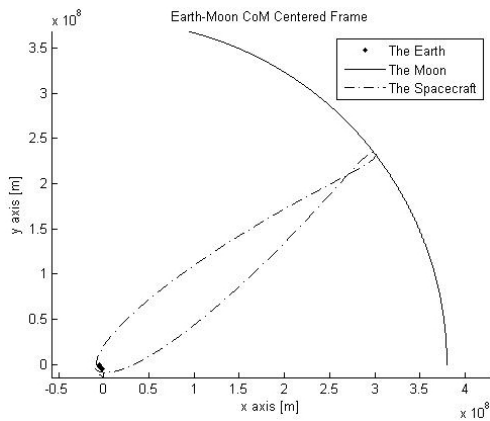|	Apollo-13	Evaluated
Initial altitude [km]	169.6088	169.6088
Lunar injection velocity [m/s]	10854.568	10967.581
Velocity change, ΔV [m/s]	3059.8872	3172.902
Resultant perimoon altitude [km]	139.7	134.0
Resultant vacuum perigee altitude [km]	129.7	129.7

Fig. 2 Earth & Moon center-of-mass centered frame.

It is important to point out the tolerance levels and the assumptions made before starting the calculations. Resultant perimoon and perigee altitude tolerances for Apollo-13, so for this paper, are $139 \pm 18.5 \, km$ and $120.5 \pm 18.5 \, km$, respectively [13]. In regard to the assumptions, firstly, except for the Sun, all celestial bodies' and the spacecraft's trajectories lie in one plane, i.e., the whole system is assumed to be planar but the Sun. Secondly, no relativistic and magnetic effects are taken into account. Finally, trajectories of all celestial bodies are considered as circular except for that of the Earth around the Sun, which makes the eccentricities zero.
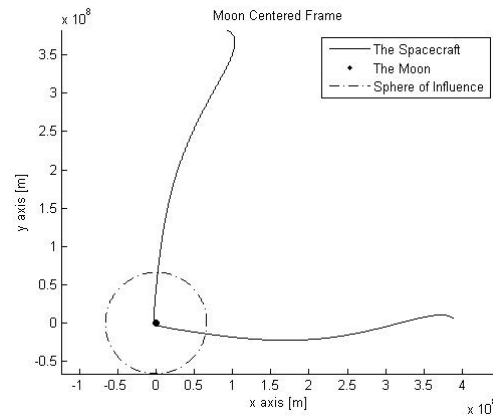

Fig. 3 Moon centered frame – Earth & Moon System

II. EFFECTS OF PERTURBATIONS ON THE FREE RETURN PATH

For a spacecraft orbiting around a central body, there are many effects acting on the satellite except for the central gravitational acceleration. These effects, named as orbital perturbations, perturb the satellite's trajectory slightly every second. Although the effects are small, they can cause a certain difference in a period of time. Perturbative effects can be originated from many factors, most common ones are atmospheric drag, non-spherical central body, solar radiation pressure (SRP) and third body gravitational effects. The orders of these perturbations at 1000 km altitude are shown in Table II [12].

Perturbative Effect	Perturbation degree
Oblateness	$10^{-2} g_0$
Solar gravity	$10^{-7} g_0$
Lunar gravity	$10^{-7} g_0$
SRP	$10^{-9} g_0$
Drag	$10^{-10} g_0$

*g_0 stands for gravity on sea level, $9.80665\ m/s^2$

It is important to highlight that the degree of some of the perturbations are strictly dependent to altitude. Drag effect for example, is the most dominant effect below 100 km, even more dominant than the central gravity. Though, as the altitude reaches 1000 km, it becomes one of the least dominant ones. Oblateness effect is one another altitude dependent effect which also decreases with altitude but not as rapid as drag. In contrast to the drag and the oblateness effects, the third body effects and SRP are much less dependent to altitude, besides, in some cases, they may get stronger with increasing altitude in case the spacecraft gets closer to the source of the perturbation. Considering a Moon mission, like in this study, lunar gravity increases and predominates that of Earth's as the spacecraft gets closer to the Moon, so it cannot be taken as a perturbative effect. In order to see the influence of the perturbative effects, separately, each of them will be included in the system.

A. Oblateness Effects

Earth's non-spherical shape causes Earth-orbiting objects to change their orbits. In order to calculate the consequences of this effect, for every planet, unitless zonal harmonic coefficients are established based on observations and experiments. Table III represents Earth's harmonic coefficients [14].

TABLE III
ZONAL HARMONICS FOR EARTH

Zonal Harmonic	Magnitude
J_1	0
J_2	1082.63×10^{-6}
J_3	-2.52×10^{-6}
J_4	-1.61×10^{-6}
J_5	-0.15×10^{-6}
J_6	0.57×10^{-6}

J_1 equals to zero means that the centers of the Earth and the spherical coordinate frame coincide. Considering rest of the harmonics, it is clear that J_2 is the most dominant one. Since after J_4, the harmonic values get ten thousandth of J_2, effects of harmonics of order of greater than 4 are mostly disregarded. Still in this paper J_5 and J_6 will be included for achieving a higher fidelity analysis. While modeling these effects, following equations are implemented:

$$\overline{p_2} = -\frac{3}{2} J_2 \frac{\mu}{r^2} \left(\frac{R_E}{r}\right)^2 \times \begin{bmatrix} \frac{x}{r}\left(1-5\left(\frac{z}{r}\right)^2\right)\hat{\imath} \\ \frac{y}{r}\left(1-5\left(\frac{z}{r}\right)^2\right)\hat{\jmath} \\ \frac{z}{r}\left(3-5\left(\frac{z}{r}\right)^2\right)\hat{k} \end{bmatrix} \quad (1)$$

$$\overline{p_3} = -\frac{1}{2} J_3 \frac{\mu}{r^2} \left(\frac{R_E}{r}\right)^3 \times \begin{bmatrix} 5\frac{x}{r}\left(7\left(\frac{z}{r}\right)^3 - 3\left(\frac{z}{r}\right)\right)\hat{\imath} \\ 5\frac{y}{r}\left(7\left(\frac{z}{r}\right)^3 - 3\left(\frac{z}{r}\right)\right)\hat{\jmath} \\ 3\left(10\left(\frac{z}{r}\right)^2 - \frac{35}{3}\left(\frac{z}{r}\right)^4 - 1\right)\hat{k} \end{bmatrix} \quad (2)$$

$$\overline{p_4} = -\frac{5}{8} J_4 \frac{\mu}{r^2} \left(\frac{R_E}{r}\right)^4 \times \begin{bmatrix} \frac{x}{r}\left(3 - 42\left(\frac{z}{r}\right)^2 + 63\left(\frac{z}{r}\right)^4\right)\hat{\imath} \\ \frac{y}{r}\left(3 - 42\left(\frac{z}{r}\right)^2 + 63\left(\frac{z}{r}\right)^4\right)\hat{\jmath} \\ -\frac{z}{r}\left(15 - 70\left(\frac{z}{r}\right)^2 + 63\left(\frac{z}{r}\right)^4\right)\hat{k} \end{bmatrix} \quad (3)$$

$$\overline{p_5} = -\frac{1}{8} J_5 \frac{\mu}{r^2} \left(\frac{R_E}{r}\right)^5 \times \begin{bmatrix} 3\frac{x}{r}\left(35\frac{z}{r} - 210\left(\frac{z}{r}\right)^3 + 231\left(\frac{z}{r}\right)^5\right)\hat{\imath} \\ 3\frac{y}{r}\left(35\frac{z}{r} - 210\left(\frac{z}{r}\right)^3 + 231\left(\frac{z}{r}\right)^5\right)\hat{\jmath} \\ 15 - 315\left(\frac{z}{r}\right)^2 + 945\left(\frac{z}{r}\right)^4 - 693\left(\frac{z}{r}\right)^6 \hat{k} \end{bmatrix} \quad (4)$$

$$\overline{p_6} = \frac{1}{16} J_6 \frac{\mu}{r^2} \left(\frac{R_E}{r}\right)^6 \times \begin{bmatrix} \frac{x}{r}\left(35 - 945\left(\frac{z}{r}\right)^2 + 3465\left(\frac{z}{r}\right)^4 - 3003\left(\frac{z}{r}\right)^6\right)\hat{\imath} \\ \frac{y}{r}\left(35 - 945\left(\frac{z}{r}\right)^2 + 3465\left(\frac{z}{r}\right)^4 - 3003\left(\frac{z}{r}\right)^6\right)\hat{\jmath} \\ -\frac{z}{r}\left(315 - 2205\left(\frac{z}{r}\right)^2 + 4851\left(\frac{z}{r}\right)^4 - 3003\left(\frac{z}{r}\right)^6\right)\hat{k} \end{bmatrix}$$
$$(5)$$

where $\bar{p}_i$ is the ith order perturbative acceleration, R_E is Earth equatorial radius (6378137 m), μ is Earth's gravitational constant ($3.9859792 \times 10^{14}\ m^3/s^2$), r is the distance from Earth's center to spacecraft's position (m) and x, y, z are the position components (m) in ECI frame.

Implementing the zonal harmonic perturbation equations, the effects of the perturbations on the trajectory now can be analyzed. Sequentially, each zonal harmonic effect was included in the calculations and corresponding differences are represented in Table IV.

TABLE IV
EFFECTS OF ZONAL HARMONICS

Zonal Harmonics	Differences [km]	
	Perimoon	Perigee
J_2	−1267.8 (crush)	-
J_3	-1.64×10^{-4}	0.0073
J_4	1.395	−26.738
J_5	-3.1×10^{-5}	5.6×10^{-4}
J_6	0.366	−7.111

Clearly, J_2 effect should inevitably be included to the calculations considering it leads spacecraft to crashing in to the Lunar surface as can be seen in Fig. 4. The dashed line represents the perturbed trajectory assuming the spacecraft

passes through the Luna with no crash. Additionally, although the J_4 effect perturbs perimoon only about $1\ km$, return perigee differs about $27\ km$ which inevitably cause the re-entry capsule to burn since the proper re-entry layer is above approximately $18\ km$. J_3's and J_5's effects do not exceed a few meters even in perigee altitude, consequently, ignoring them will not cause any failures. In regard to J_6, though the effect does not cause any fatalities as the resultant altitudes stay in the tolerance levels, the effect is alarmingly high as it differed the perigee more than 7 km. Correspondingly, taking into account J_6 leads safer and more accurate calculations indisputably. Because the 6th order harmonic effect causes a difference within the tolerance levels, for higher ordered terms, presumably the effects will diminish and be ignorable. Thus, no order higher than 6th will be analyzed in this study.
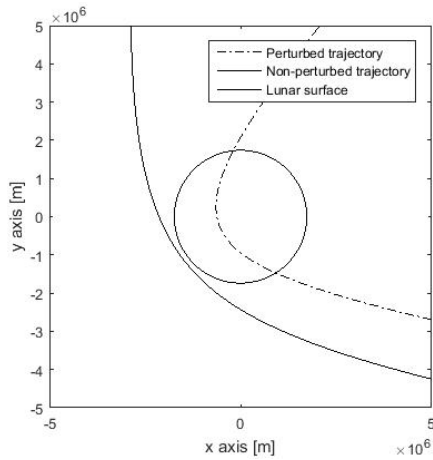

Fig. 4 J_2 effect on Lunar flyby

B. Atmospheric Drag

Even though most of the atmosphere is below 100 km (more than 99.9999%), it can cause satellites to deorbit considering orbital velocity of satellites is approximately 8 km/s which increases the drag effect excessively. In order to model the drag effect, US Standard Atmosphere 1976 model was employed to determine air density. The drag force was obtained with commonly known formulation given in (6) [12]:

$$\bar{a}_{aero} = -\frac{1}{2}\frac{\rho_{air}}{m}\ V_{rel}^2\ C_D\ A_{Ref}\frac{\bar{V}_{rel}}{V_{rel}} \tag{6}$$

where $\bar{F}_{aero}$ is the drag force vector (N), ρ_{air} is the air density (kg/m³), m is the spacecraft mass (kg), V_{rel} is the relative air velocity magnitude (m/s), $\bar{V}_{rel}$ is the relative air velocity vector (m/s), C_D is drag coefficient and A_{Ref} is the reference area (m²).

As instead of a finite burn, an instantaneous thrust is applied, couple of assumptions in modelling the drag must be used. At the beginning of the S-IVB ignition which lasts 350.8 s [11], mass of the spacecraft was 164 tons and at the burnout 57.4 tons, approximately [11]. Half of the sum of ignition and burn-out masses would be considered as constant mass in most of the cases; however, this is a unique case

which requires certain out of ordinary factors to be accounted for. Firstly, there will be no drag at excessively high portion of the flight and beyond 1000 km it is safe to ignore the drag force. Secondly, most of the drag will be experienced at the first few minutes of the flight where the atmosphere is still relatively thick and the spacecraft is massy. Hence, it is more reasonable to implement a weighted average instead of the arithmetic average. As a result, with a rough weighting, 120 tons, was used for the calculations. A reference area of 34.285 m² [15] is taken together with a drag coefficient of 2.2 which is common usage for space vehicles regardless to shape of the vehicle in low Earth orbit [16].

Running the simulation with the drag effect, perimoon and perigee altitudes differed -1.046 km and 19.617 km, respectively. Since the perturbed perigee is about 10 km above the acceptable layer and high enough for the spacecraft to skip over the atmosphere, it is clear the atmospheric drag must be considered in such a mission.

C. Third Body Effects

Celestial bodies in the Solar system, although the distances are great, have effect on spacecrafts, orbiting around Earth thanks to their enormous masses. The Sun and the Moon predominantly have a similar amount of effect since their masses and squared distances are proportional. On the other hand, planets and other celestial bodies perturb trajectories rather, at some limited level. In order to calculate these effects, it is necessary to determine the position vectors of regarding celestial body with respect to the Earth and the spacecraft. Fortunately, the positions of the celestial bodies are strictly dependent to time and having known the time, the positions can be determined accurately. An appropriate time format for Astronautical applications is Julian date format that facilitates calculations significantly. The following procedure is one of the simplest methods among time conversions from Universal Time Coordinated (UTC) to Julian date [12]:

$$JD = J_0 + \frac{UT}{24} \tag{7}$$

where JD is the Julian date, J_0 is the Julian day number and UT is the Universal time which can be obtained by (8) and (9), respectively.

$$J_0 = 367y - INT\left\{\frac{7\left[y + INT\left(\frac{m+9}{12}\right)\right]}{4}\right\} + INT\left(\frac{275m}{9}\right) + d + 1721013.5 \tag{8}$$

noting y is the year number ($1901 \le y \le 2099$), m is the number of the months ($1 \le m \le 12$), d is the number of the days ($1 \le d \le 31$) and INT is the integer operator.

$$UT = hh + \frac{mm}{60} + \frac{ss}{3600} \tag{9}$$

where hh is hours, mm is minutes and ss is seconds.

1) Solar Gravity

Sun position vector is the first step of the calculation of

solar gravity together with the solar mass information which can easily be found in astronautical resources. Solar position vector as a function of time based on Astronautical Almanac can be found with the following algorithm [12]:

$$\lambda = L + 1.915° \sin(M) + 0.020° \sin(2M) \qquad (10)$$

where λ is the Solar ecliptic longitude ($0° \leq \lambda \leq 360°$), L and M are mean longitude ($0° \leq L \leq 360°$) and mean anomaly ($0° \leq M \leq 360°$).

$$L = 280.459° + 0.98564736°n \qquad (11)$$

$$M = 357.529° + 0.98560023°n \qquad (12)$$

noting n is the day number since J2000 and evaluated by:

$$n = JD - 2451545 \qquad (13)$$

Having obtained the angles, magnitude of the Sun position vector can be determined by:

$$R_s = (1.00014 - 0.01671 \cos(M) - 0.000140 \cos(2M))AU \qquad (14)$$

where R_s is the magnitude of Sun position vector (km) and AU is Astronautical Unit ($149597870.691\ km$). To get the position vector, following conversion from geocentric ecliptic frame to geocentric equatorial frame must be done:

$$\{\bar{u}_s\}_{XYZ} = [R_1(-\epsilon)]\{\bar{u}_s\}_{X'Y'Z'}$$
$$= \begin{bmatrix} 1 & 0 & 0 \\ 0 & \cos\epsilon & -\sin\epsilon \\ 0 & \sin\epsilon & \cos\epsilon \end{bmatrix} \begin{Bmatrix} \cos\lambda \\ \sin\lambda \\ 0 \end{Bmatrix} = \begin{Bmatrix} \cos\lambda \\ \cos\epsilon.\sin\lambda \\ \sin\epsilon.\sin\lambda \end{Bmatrix} \qquad (15)$$

where ϵ is the obliquity (°), $\{\bar{u}_s\}_{XYZ}$ is the unit vector of Sun position in geocentric equatorial frame and $\{\bar{u}_s\}_{X'Y'Z'}$ is the unit vector of Sun position in geocentric ecliptic frame.

$$\epsilon = 23.439° - 3.56 \times 10^{-7}n \qquad (16)$$

$$\bar{R}_s = R_s\{\bar{u}_s\}_{XYZ} \qquad (17)$$

Equation (17) completes the Sun position vector calculation and finally the gravitational attraction of Sun can be found. The perturbative acceleration due to Solar gravity can easily be found with Newton's universal law of gravitation:

$$\bar{a}_s = \mu_s \left(\frac{\bar{R}_{S/sc}}{R_{S/sc}^3} - \frac{\bar{R}_S}{R_S^3} \right) \qquad (18)$$

Here, $\bar{a}_s$ is the solar perturbative acceleration, μ_s is Solar gravitational constant ($1.327124400 \times 10^{20}$ m³/s²), $\bar{R}_{S/sc}$ and $\bar{R}_S$ Sun position vectors with respect to spacecraft and Earth (m), accordingly, $R_{S/sc}$ and R_S are the magnitudes as well.

In Fig. 5, the circle with a dot in the middle stands for Sun, and letter "s" for spacecraft. Also, since the relativistic effects are ignored, apparent and real Sun positions are identical.

In the calculations, Sun, Earth and Moon placed similarly at their relative positions. It should be underlined that the perturbative effect of the Solar gravity should be applied both to the spacecraft and to the Moon. Equation (18) is employed to calculate the solar gravitational perturbation on the Moon rearranging only $R_{S/sc}$ with $R_{S/m}$ which stands for the Sun's position with respect to the Moon.
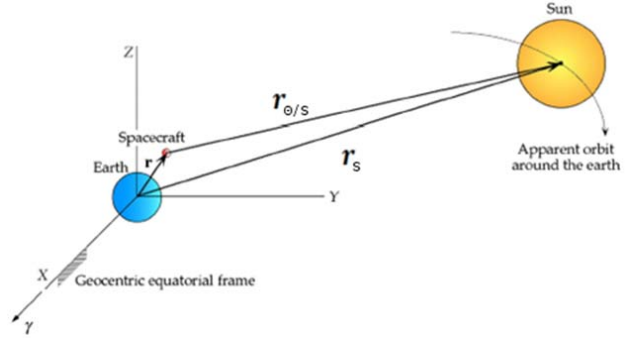

Fig. 5 Sun vectors with respect to Earth and spacecraft [12]

Including the Solar gravity effect, an apparent difference occurred as can be seen from Fig. 6. The altitudes differed $225.17\ km$ and $23433\ km$ for perimoon and perigee, therefore not to question, the effect cannot be disregarded. Also, it is good to note the difference level may vary in a wide range with different positioning of celestial bodies; nonetheless, the variance does not change the quality of the effect.
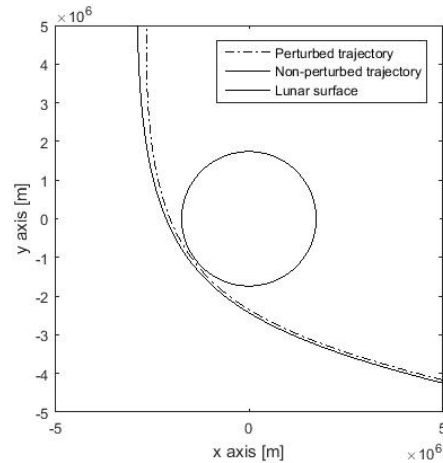

Fig. 6 Solar gravity effect on Lunar flyby

2) Jovian and Other Planetary Gravities

Before investigating all planets, it is better to start with the most dominant one, Jupiter. In case its effect is found to be unnecessary, effects of the rest become so, together with it. To maximize the Jovian gravitational effect, regardless to the real positions, possible closest distances are chosen (4.2 AU). Also for simplification in computations, Jupiter's position is fixed in space since its true anomaly changes only about 0.5° during

the mission period.

Similar procedure to the solar gravity was followed in the Jovian gravity calculation. Replacing $R_{s/sc}$ with $R_{j/m}$ in (18) which stands for Jupiter's position with respect to the Moon, we get:

$$\bar{a}_j = \mu_j \left(\frac{\bar{R}_{j/sc}}{R_{j/sc}^3} - \frac{\bar{R}_j}{R_j^3} \right) \tag{19}$$

where $\bar{a}_j$ is the Jovian perturbative acceleration, μ_j is the gravitational constant of Jupiter ($1.26686638 \times 10^{27} \, \mathrm{m^3/s^2}$), $\bar{R}_{j/sc}$ is Jovian position vector with respect to spacecraft (m) and $\bar{R}_j$ is constant Jovian position vector with respect to Earth (m), $R_{j/sc}$ and R_j are the magnitudes as well.

Simulation started with the initial conditions corresponding to the unperturbed system's initial conditions. Resultant altitudes differed -1 meter in perimoon and 15 meters in perigee. Clearly, differences are small enough to be neglected even for a closest pass. This shows that together with Jupiter, gravitational effects of all other planets can be ignored for a Moon mission.

B. Solar Radiation Pressure

One another effect of the Sun is SRP. As objects in space are illuminated, a pressure difference occurs between illuminated and shadowed surfaces. Though the photons have no mass, they do have momentum transferred electromagnetically, which causes satellites to change trajectory gradually. This phenomenon is denoted as SRP. Of course this tiny effect is only countable if the satellite is exposed for a sufficient period of time. In a lunar mission, which lasts nearly a week, the period probably is long enough to observe certain differences.

Before modelling SRP, Sun position must be known together with the solar pressure level at 1 AU. Fortunately, in section C−1) Solar Gravity, Sun position as a function of time was derived, also, solar pressure level at 1 AU is known in the literature. The equation used to obtain SRP is given [17]:

$$\bar{a}_{\mathrm{SRP}} = -\frac{P_{SR} C_R A_{\mathrm{Sun}}}{m} \{\bar{u}_s\}_{XYZ} \tag{20}$$

where $\bar{a}_{\mathrm{SRP}}$ is the perturbative acceleration caused by SRP ($\mathrm{m/s^2}$), P_{SR} is the solar pressure at 1 AU ($4.56 \, \mu\mathrm{Pa}$), C_R is the reflectivity coefficient taken as 1.6 in this study, A_{Sun} is area exposed to the Sun ($\mathrm{m^2}$) and $\{\bar{u}_s\}_{XYZ}$ is the unit sun vector.

Considering the Apollo-13 mission, Command Module, Service Module and Lunar Module are roughly 16 m long, in total, and have a 4.25 m mean diameter, A_{Sun} is taken as $65 \, \mathrm{m^2}$ and the total mass is taken as 44100 kg [15]. Through the flight, the spacecraft goes into shadows of both the Moon and the Earth where no SRP is exposed. Earth's shadow is taken into account by checking if there is line of sight between the Sun and the spacecraft or not. On the other hand, time spent in the shadow of the Moon, which is around 16 minutes, was relatively short compared to the total mission time; hence, it was neglected [18].

TABLE V
PERTURBATION EFFECTS ON PERIAPSIDES

Perturbative effect		Differences [km]		Level
		Perimoon	Perigee	
Oblateness effects	J_2	-1268	$-$	3
	J_3	-1.6×10^{-4}	0.0073	1
	J_4	1.395	-26.738	3
	J_5	-3×10^{-5}	5×10^{-4}	1
	J_6	0.366	-7.111	2
Atmospheric drag	-	-1.046	19.617	3
Third body effects	Solar	225.17	23433	3
	Jovian	-1	15	1
SRP	-	0.382	-6.802	2

Starting the model with SRP effect, perimoon and perigee altitudes varied 0.382 km and -6.802 km. Differences are not fatal and the altitudes are in the tolerance levels, though, similar to J_6, SRP effect is threateningly strong and must be considered. For instances where the spacecraft is planned to be in shadow for greater durations than for this case, the effect could get small enough to be ignored, still, it is better to monitor the variations in the trajectory.

III. CONCLUSION

In this paper, starting with a perturbation free lunar figure-8 trajectory, the effects of common perturbations on the trajectory are investigated. Regarding with the magnitude of the effects, levels of perturbations are discussed in terms of both quality and quantity as summarized in Table V. Level 1, level 2, and level 3 are standing for negligible, significant and fatal, accordingly, and, it is concluded that level 2 and level 3 effects must inevitably be considered planning a Moon mission. Even though level 2 effects do not exceed the mission tolerances, combination of them have the potential to exceed. J_2 and J_4 apparently cause fatalities together with atmospheric drag and solar gravity. J_6 and SRP based differences remain within the tolerances, yet, the differences are significant enough that, they cannot be omitted. Remaining effects, namely J_3, J_5 and Jovian gravity effects are found to be unnecessary along with the other planetary gravities since the Jupiter is the most dominant one.

REFERENCES

[1] European Space Agency, "Helium-3 mining on the lunar surface". Accessed on November 15, 2016. Retrieved from http://www.esa.int/Our_Activities/Preparing_for_the_Future/Space_for_ Earth/Energy/Helium-3_mining_on_the_lunar_surface.

[2] I. Crawford, "Moon village", *Astronomy & Geophysics*, vol. 58, no. 6, pp. 6.18-6.21, 2017.

[3] K. Tate, "Home on the Moon: How to build a lunar colony", 2013, accessed on April 25, 2019. Retrieved from https://www.space.com/21588-how-moon-base-lunar-colony-works-infographic.html

[4] Solar System Exploration Research Virtual Institute, "*Chandrayaan-2 to land two rovers*", accessed on December, 2016, retrieved from https://sservi.nasa.gov/articles/chandrayaan-2-to-land-two-rovers

[5] B. Cohen, and R. Staehle, "Lunar flashlight", Solar System Exploration Research Virtual Institute, accessed on December, 2016, retrieved from https://sservi.nasa.gov/articles/lunar-flashlight

[6] B. A. Cohen, J. A. Bassler, J. M. McDougal, D. W. Harris, L. Hill, M. S. Hammond, B. J. Morse, C. L. B. Reed, K. W. Kirby and T. H. Morgan, "The international lunar network (ILN) anchor nodes mission update", *40th Lunar and Planetary Science Conference*, Jan., 2009.

[7] R. D. Adamo, "Apollo-13 trajectory reconstruction via state transition matrices", *Journal of Guidance, Control, and Dynamics*, vol. 31, no. 6, pp. 1772-1781, 2008

[8] M. Jesick and C. Ocampo, "Symmetric lunar free-return trajectories", *Journal of Guidance, Control, and Dynamics,* vol 34, no. 1, pp. 98-106, (2011).

[9] J. Li, S. P. Gong, H. Baoyin and F. Jiang, "Lunar orbit insertion targeting from the two-segment lunar free-return trajectories", *Advances in Space Research*, vol. 55, no. 4, pp 1051-1060, 2015.

[10] E. Unal, "Free return trajectories to Moon", *9th International Conference on Recent Advances in Space Technologies*, Istanbul, June, 2019.

[11] National Aeronautics and Space Administration, "Apollo 13 Mission Report", Houston, Texas, 1970.

[12] H. D. Curtis, *Orbital Mechanics for Engineering Students*, 3rd ed., Elsevier , Waltham, Massachusetts, USA, 2010, ch .12.

[13] B. Michaels, "Exploration of lunar free-return trajectories", unpublished, accessed on November 6, 2017. retrieved from http://ccar.colorado.edu/asen5050/projects/projects_2012/michels/

[14] H. Schaub and J. L. Junkins, *Analytical Mechanics for Aerospace Systems*. AIAA education series, 2002, pp. 372-380.

[15] National Aerospace and Space Administration, "Apollo 13 Press Kit", Washington DC, 1970.

[16] D. M. Prieto, B. P. Graziano and P. C. E. Roberts, "Spacecraft drag modelling", *Progress in Aerospace Sciences*, vol. 64, pp. 56-65, 2014.

[17] C. Colombo, C. Bewick, and C. McInnes, "Orbital dynamics of high area-to-mass ratio spacecraft under the influence of j2 and solar radiation pressure", *62nd International Astranautical Congress,* Cape Town, 2011.

[18] National Aeronautics and Space Administration, "Apollo 13 technical air-to-ground voice transcript". Manned Spacecraft Center. Houston, Texas, 1970.